A Wideband Fast Integral Equation Solver Combining Multilevel Fast Multipole and Multilevel Green's Function Interpolation Method with Fast Fourier Transform Acceleration

Dennis T. Schobert and *Thomas F. Eibert*
Lehrstuhl für Hochfrequenztechnik Technische Universität München
Arcisstr. 21, 80333 München, Munich, Germany
schobert@ieee.org

Abstract

A wideband fast integral solver employing a fast Fourier transform accelerated multilevel Green's function interpolation method (MLIPFFT) combined with the multilevel fast multipole method (MLFMM) is presented. On fine levels of the employed oct-tree structure, the low frequency stable MLIPFFT is utilized. At a certain wavelength dependent threshold for the box size, the interpolation point based representation of the MLIPFFT is converted into its $\hat{k}$-space representation suitable for an MLFMM. On the coarser levels, MLFMM translations are used then, where the MLIPFFT becomes less efficient. The functionality of this hybrid algorithm is demonstrated in an example.

1 Introduction

Method of moment (MoM) based surface integral equation techniques are among the most popular methods for solving electromagnetic radiation and scattering problems. By MoM, the respective surface integral operators are converted into matrix-vector products. For compression of the corresponding fully-populated system matrix, fast integral solvers have been developed over the past years, which reduce the numerical complexity of the corresponding matrix-vector products. A very effective fast integral solver is the multilevel fast multipole method (MLFMM). This method works with a multipole series expansion of the respective Green's functions in combination with a plane wave expansion. For low frequencies, the suitability of the MLFMM is restricted since it suffers a low-frequency breakdown [1], which is due to numerical difficulties in the evaluation of the translation operators. Especially for EMC problems, low-frequency stability is, however, mandatory and it would even be desirable to have wideband solvers, which work over wide frequency bands. To overcome the low-frequency problem, it is possible to work with the standard multipole expansion and without diagonalization [2]. Another possibility is the inclusion of evanescent waves to better capture reactive fields at low frequencies [3]. A common property of all these methods is that they work with field expansions with respect to a common expansion origin in the corresponding source and observation groups. This results in approximation errors, which are small close to the origins and increase with distance to the expansion origins. Conceptually similar to this are Taylor expansions of the Green's functions as utilized in the so-called *accelerated Cartesian expansion method* [4].

A different approach is followed by methods, which work with several matching locations in the source and observation regions leading to a rather constant approximation error throughout the approximation domain. One example following this philosophy is the *adaptive integral method* (AIM) working with a projection of the basis functions on a regular grid of sources [5]. Since this projection leads to accurate results only for far-interactions, the near-interactions must be computed by explicit integration. A serious shortcoming of classical AIM in this respect is its difficulty to distinguish between near-range and far-range leading to the necessity of a calibration or pre-correction step as also found in the pre-corrected FFT methods [6, 7]. An interesting implementation of an AIM-like method is found in [7], where the mapping from the irregular basis functions to the regular grid of sources is accomplished by Lagrange interpolation. Another important shortcoming of the AIM-like methods is that their regular grid of sources covers a fully cuboid domain, which does often cover large portions of empty space leading to a large amount of unnecessary computations. This problem is overcome by hierarchical representations with an oct-tree structure as known from MLFMM and as e.g. discussed in [8]. These methods are particularly useful but not restricted to low frequency problems. However, for higher frequencies the number of interpolation points must be increased in three dimensions for coarser levels in order to capture the oscillatory behavior of the Green's functions.

978-1-4244-6051-9/11/$26.00

In this work, we present an efficient wideband hybrid algorithm, which works with MLFMM based coupling computation on coarse levels and MLIPFFT based coupling computation on fine levels in order to avoid the low-frequency breakdown of the MLFMM. In contrast to the method presented in [9], the interpolation point interactions are computed utilizing an FFT-based acceleration. Furthermore, standard dyadic MLFMM translation operators can be used by employing a direct field surface integral equation.

2 Surface Integral Equations

Consider a MoM discretized and time-harmonic surface integral equation (IE)

$$[Z_{mn}]\{I_n\} = \{b_m\}, \qquad m,n = 1,...,N_I \tag{1}$$

with suppressed time dependence $e^{j\omega t}$ for the computation of electromagnetic scattering and radiation problems of *perfectly electric conducting* objects. The N_I unknown electric surface current expansion coefficients I_n are introduced according to

$$\boldsymbol{J}_A(\boldsymbol{r}) = \sum_{n=1}^{N_I} I_n \boldsymbol{\beta}_n(\boldsymbol{r}). \tag{2}$$

b_m are the excitation vector elements due to an incident plane wave or due to delta-gap voltage sources (see e.g. [1]). The $\boldsymbol{\beta}_n(\boldsymbol{r}) = (\boldsymbol{r} - \boldsymbol{r}_c)/(2A)$ are *Rao-Wilton-Glisson* vector basis functions on triangular meshes, where A is the area of the corresponding triangle and $\boldsymbol{r}_c$ is one of the triangle's vertices. The excitation vector elements are given as

$$b_m = -\iint\limits_A [\boldsymbol{\beta}_m(\boldsymbol{r}) \cdot \boldsymbol{E}^{inc}(\boldsymbol{r})] da \tag{3}$$

with the electric field strength $\boldsymbol{E}^{inc}(\boldsymbol{r})$ of the respective excitation. The respective system matrix entries are computed by

$$Z_{mn} = -j\omega\mu \iint\limits_A \left[\boldsymbol{\beta}_m(\boldsymbol{r}) \cdot \iint\limits_{A'} \left(\overline{\boldsymbol{I}} + \frac{1}{k^2}\nabla\nabla \right) G(\boldsymbol{r},\boldsymbol{r'}) \cdot \boldsymbol{\beta}_n(\boldsymbol{r'}) da' \right] da \tag{4}$$

for far range computations. $G(\boldsymbol{r},\boldsymbol{r'}) = e^{-jk|\boldsymbol{r}-\boldsymbol{r'}|}/(4\pi|\boldsymbol{r}-\boldsymbol{r'}|)$ is the scalar Green's function of the Helmholtz equation. Furthermore, μ and k are the permeability and wave number of the solution domain.

3 Lagrange Interpolation of the Green's Function

For the solution of (4), the dyadic Green's function is at first factorized by *Lagrange interpolation* with respect to source and test domain:

$$\tilde{Z}_{mn} = -j\omega\mu \sum_{i=1}^{N_p^3} \iint\limits_A \mathcal{L}_i(\boldsymbol{r}) \boldsymbol{\beta}_n(\boldsymbol{r}) da \cdot \sum_{j=1}^{N_p^3} \left(\overline{\boldsymbol{I}} + \frac{1}{k^2}\nabla\nabla \right) G(\boldsymbol{r}_i,\boldsymbol{r'}_j) \cdot \iint\limits_{A'} \mathcal{L}_j(\boldsymbol{r'}) \boldsymbol{\beta}_n(\boldsymbol{r'}) da'. \tag{5}$$

$\mathcal{L}_j(\boldsymbol{r'})$ and $\mathcal{L}_i(\boldsymbol{r})$ are the appropriate 3D Lagrange interpolation factors of the source and test domain and N_p is the number of interpolation points per dimension. The integrals can now be precomputed and do not have to be computed again in every matrix vector product of an iterative linear equation system solver. In [8] it has been shown that this kind of formulation has increased robustness for interpolatory methods as compared to the more common mixed potential formulation (i.e. [4, 9]).

4 Diagonalization of the Translation Operator

A drawback of the former mentioned formulation is that the computational effort for the far-interaction computation increases with the number N_p of interpolation points by the power of 6, as a three dimensional interpolation is necessary for the consideration of arbitrarily shaped surfaces. Furthermore, the translation operators are still full. The convolutional properties of the Green's functions are utilized in order to diagonalize the full operator by an FFT and to evaluate it by a simple Hadamard product in the diagonal FFT domain. It is obvious that this FFT acceleration gains numerical efficiency with an increase of interpolation points. However, it is found that even for 3 interpolation points per dimension (quadratic interpolation) this approach is more effective than direct translation in space-domain.

5 Multilevel Scheme

In contrast to techniques like AIM with one single regular grid for the whole domain of a scattering object, an oct-tree multilevel structure similar to that of the well-known MLFMM is used. This cubic group structure allows to perform translations between non-empty boxes, only. Dependent on the ratio a^{lev}/λ of the respective cubic group's side length a^{lev} on a certain level to the wavelength λ, different strategies are followed. On fine levels with box side lengths smaller than a threshold r^{const}, MLIPFFT interaction computations are performed. If the side length at the next coarser level $lev+1$ is still below the threshold r^{const}, the source contributions are anterpolated to a regular grid with identical N_p in the coarser level cube with side length $a^{\text{lev}+1} = 2a^{\text{lev}}$. For the finest level $levtrans$ fulfilling the condition $a^{levtrans} \geq r^{\text{const}}$, a transition between the interpolation point based MLIPFFT formulation to the MLFMM based spectral representation is performed according to

$$\tilde{Z}_{mn}^{levtrans} \approx -j\frac{\omega\mu}{4\pi}\sum_{i=1}^{N_p^3}\oiint\left\{\boldsymbol{S}_{i,m}T_{\text{map}}^{*}(\boldsymbol{r}_{im'})\cdot\sum_{j=1}^{N_p^3}T_L(\hat{k}\cdot\hat{r}_{m'n'})(\overline{\boldsymbol{I}}-\hat{k}\hat{k})\cdot\boldsymbol{S}_{j,n}T_{\text{map}}(\boldsymbol{r}'_{jn'})\right\}d\hat{k}^2 \tag{6}$$

where r^{const} is chosen sufficiently large in order to avoid the MLFMM low-frequency breakdown. m' and n' denote the source and test group centers, $T_{\text{map}}(\boldsymbol{r}) = e^{j\boldsymbol{k}\cdot\boldsymbol{r}}$ is the respective mapping operator between the MLIPFFT interpolation point vector amplitudes $\boldsymbol{S}_{i,m}$ or $\boldsymbol{S}_{j,n}$ and MLFMM plane waves. Also, $T_L(\hat{k}\cdot\hat{r}_{m'n'})(\overline{\boldsymbol{I}}-\hat{k}\hat{k})$ is the standard dyadic MLFMM translation operator to be found e.g. in [1]. For all subsequent coarser levels, computations are performed according the MLFMM procedure. Due to the underlying direct field integral equation, 2 instead of 4 complex multiplications for every single coupling computation within the MLFMM part are sufficient when compared to a mixed potential formulation.

6 Numerical Example

The numerical efficiency of the presented algorithm is demonstrated for a bistatic RCS computation. The computation has been performed on one core of a 64-Bit PC (Intel quad core CPU with 2.83 GHz clock speed, 16 GB RAM). As linear equation system solver, a Generalized Minimal Residual (GMRES) solver with Given's rotations has been used. The combined MLIPFFT/MLFMM solution was found within 5 100 sec and with a total memory consumption of 938 MByte. The MLIPFFT needed 5 448 sec with 1 250 MByte of memory and the MLFMM solution was found within 5 394 sec with a memory demand of 1 930 MByte. The respective results show prefect matching (Fig. 1). Due to the low solution time and memory demand, the combined MLIPFFT/MLFMM is the method of choice.

7 Conclusions

A combined MLIPFFT/MLFMM solver for wideband problems, which are typical for EMC analysis, has been presented. For MLIPFFT, the originally full translation operators are diagonalized by a 3D FFT. For coarse levels, the MLIPFFT interpolation points are used to generate the MLFMM $\hat{k}$-space representation. The high numerical efficiency of this hybrid algorithm was shown in a numerical example.

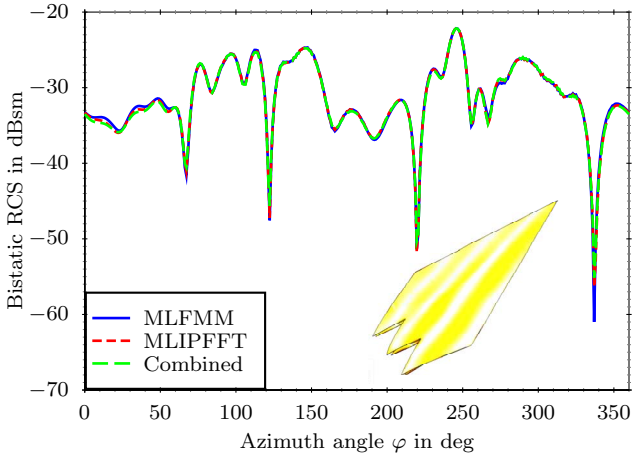

Figure 1: Comparison of bistatic RCS computations performed by MLFMM, MLIPFFT and combined MLIPFFT/MLFMM.

References

[1] W. C. Chew, J. Jin, E. Michielssen, and J. Song, *Fast and Efficient Algorithms in Computational Electromagnetics*. Boston, MA: Artech House, 2001.

[2] J.-S. Zhao and W. C. Chew, "Integral equation solution of Maxwell's equations from zero frequency to microwave frequencies," *IEEE Trans. Antennas Propag.*, vol. 48, no. 10, pp. 1635–1645, Oct 2000.

[3] L. J. Jiang and W. C. Chew, "Low-Frequency Fast Inhomogeneous Plane-Wave Algorithm (LF-FIPWA)," *Microw. Opt. Technol. Lett.*, vol. 40, no. 2, pp. 117–122, Jan 2004.

[4] M. Vikram, H. Huang, B. Shanker, and T. Van, "A Novel Wideband FMM for Fast Integral Equation Solution of Multiscale Problems in Electromagnetics," *IEEE Trans. Antennas Propag.*, vol. 57, no. 7, pp. 2094–2104, July 2009.

[5] E. Bleszynski, M. Bleszynski, and T. Jaroszewicz, "AIM: Adaptive Integral Method for Solving Large-Scale Electromagnetic Scattering and Radiation Problems," *Radio Sci.*, vol. 31, pp. 1225–1251, 1996.

[6] S. D. Gedney, A. Zhu, W.-H. Tang, G. Liu, and P. Petre, "Fast High-Order Quadrature Sampled Pre-Corrected FFT for Electromagnetic Scattering," *Microw. Opt. Techn. Let.*, vol. 35, no. 5, pp. 343–349, Mar 2003.

[7] S. M. Seo and J.-F. Lee, "A Fast IE-FFT Algorithm for Solving PEC Scattering Problems," *IEEE Trans. Magn.*, vol. 41, no. 5, pp. 1476–1479, May 2005.

[8] D. T. Schobert, T. F. Eibert, and C. H. Schmidt, "Fast Fourier Transform Accelerated Multilevel Green's Function Interpolation for Mixed Potential and Direct Field Surface Integral Equations," in *EuCAP 2011*, Apr. 2011.

[9] M. Chen, R. Chen, X. Hu, Z. Fan, and D. Ding, "Augmented MLFMM for Solving the Electromagnetic Scattering Problems with Fine Structures," in *2010 International Conference on Microwave and Millimeter Wave Technology (ICMMT)*, May 2010, pp. 603 –606.